Enhancement of Cd^{2+} removal from aqueous solution by multifunctional mesoporous silica: Equilibrium isotherms and kinetics study

Farzad javaheri[1], Zeinab Kheshti[1], Soheila Ghasemi[2], Ali Altaee*[3]

[1]Department of Chemical Engineering, School of Chemical and Petroleum Engineering, Shiraz University, Shiraz 7193616511, Iran.

[2]Department of Chemistry, College of Sciences, Shiraz University, Shiraz 7194684795, Iran

[3]School of Civil and Environmental Engineering, University of Technology Sydney, Ultimo, NSW 2007, Australia

Abstract

In this work, a novel amino-functionalized mesoporous microsphere was synthesized to remove cadmium ions from water. The Fe_3O_4@SiO_2@*m*-SiO_2–NH_2 micro-spheres were successfully prepared *via* a facile two-stage process by coating of the as-synthesized magnetic cores with a silica shell followed by increasing the porosity of the structure using a cationic surfactant as structure-directing agents. The template removal from the structure has been performed following the method of solvent extraction and methanol-enhanced supercritical fluid CO_2 (SCF-CO_2) extraction. This novel approach provides the multifunctional microspheres with a high surface area, which improves the adsorption capacity of adsorbent. Characterization of the as-synthesized adsorbent were analytically determined showing that as-prepared adsorbent has a significant surface area of 637.38 m^2 g^{-1}. The kinetic data agreed with pseudo-second-order model and Langmuir isotherm. The maximum adsorption capacity of the synthesized adsorbent was about 884.9 mg g^{-1}, and can be easily separated from solution under an external magnetic field. The synthesized microspheres were recycled using HCl and cadmium removal was over 92% after 6 cycles, which confirms the chemical stability and reusability of the manufactured particles.

* Ali.Altaee@uts.edu.au

Highlights

- A novel amino-functionalized mesoporous microsphere with a core-shell structure was synthesized.
- The adsorbent has 637.383 m^2 g^{-1} specific surface area and 884.906 mg g^{-1} adsorption capacity.
- The adsorbent removed more than 90% of the cadmium ions from an aqueous solution.
- The microspheres were easily separated from the solution by a magnet and recycled for six times.

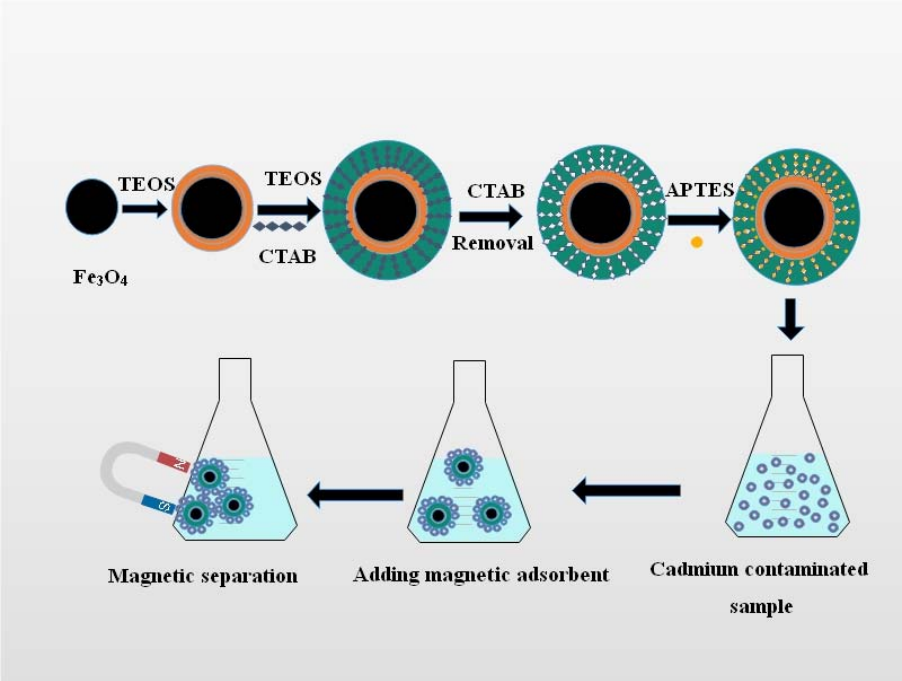

Graphical abstract. Synthesis of Fe_3O_4@SiO_2@*m*-SiO_2–NH_2 micro-spheres and cadmium removal procedure

Keywords:

Magnetic nanoparticles; amino-functionalized microspheres; Mesoporous silica; core-shell; Cadmium removal

1. Introduction

Heavy metals contamination of water resources has always been a major environmental concern [1] for being toxic and carcinogenic pollutants, which can congregate in living organisms and directly enter the food chain [2]. Toxic heavy metals like cadmium (Cd), arsenic (As), lead (Pb), mercury (Hg), chromium

(Cr), zinc (Zn), copper (Cu) and nickel (Ni) have been reported as the main pollutants in water reservoirs[3, 4]. Such contaminants can disrupt the enzymatic systems of humans and animals and threaten their health [3]. Cadmium is one of the most hazardous metals, which has dangerous effects on the environment and human. It discharges directly or indirectly to the environment through industrial wastewaters like mining, Cd-Ni batteries, metal plating industries, phosphate fertilizer, stabilizers and alloys [4]. The accumulation of cadmium ions in the human body, especially inside kidneys, may lead to dysfunction of these organs. Destruction of red blood cells and testicular tissue, lung disease and high blood pressure are other effects of cadmium poisoning in humans [5, 6]. Because of the serious effects of cadmium pollution, the World Health Organization has considered 0.005 mg L^{-1} as the allowable concentration for cadmium in drinking water. One of the most important measuring in water purification is the progress of an effective procedure for eliminating cadmium ions from the aqueous medium to prevent any harmful damage to the environment and ecological system. [7].

Adsorption, reverse osmosis, solvent-based extraction, membrane processes, ion exchange, evaporation, and chemical precipitation are common methods for removing heavy metals such as cadmium from contaminated water. [3, 8-11]. Most of these approaches are not economic and generate a considerable amount of sludge. On contrary, adsorption has been widely used by researchers because of its simplicity, applicability, cost-effectiveness, insensitivity to pollutants, lack of toxic compound formation and the possibility of recycling for reuse [12]. Yaacoubi *et al.* [13] removed cadmium ions from aqueous mixtures by utilizing natural phosphate as an adsorbent. The adsorption capacity of natural phosphate was 26.6 mg g^{-1} at pH of 5.0. Khezami *et al.* [14] synthesized zinc oxide (ZnO) nanoparticles for cadmium removal from aqueous solution. The adsorption capacity of ZnO nanoparticles to Cd^{2+} was 217.4 mg g^{-1} at 328 K. Ge *et al.* [15] used Fe_3O_4@APS@AA-*co*-CA nanoparticles to remove heavy metal ions (Cu^{2+}, Cd^{2+}, Pb^{2+}, Zn^{2+}) from water. The adsorbent had the adsorption capacity of 126.9, 29.6, 166.1 and 43.4 mg g^{-1} for Cu^{2+}, Cd^{2+}, Pb^{2+} and Zn^{2+}, respectively. Khiadani *et al.* [16] used iron oxide nanoparticles under a magnetic field to improve urban run-off quality. They reported the average removal efficiency of 41.5, 93.9, 96.2, 88.4 and 87.4 % for turbidity, Pb, Zn, Cd, and phosphate, respectively. Zhang *et al.* [17] used magnetic particles coated with polyacrylic acid to treat practical paper factory wastewater. They removed up to 76 % of COD from the wastewater.

Among several kinds of adsorbent, eco-friendly magnetic nanoparticles (MNPs) have attracted a lot of attention due to their simple separation from solutions by an external magnetic field [18]. However, MNPs can be destroyed in acidic and corrosive conditions and hence they are often protected with an inorganic shell such as silica. Previous studies suggested that coating Fe_3O_4@SiO_2 with a mesoporous silica shell increases the surface area and provides better adsorption capacity [19-21]. To synthesis the mesoporous

silica shell, organic templates must be extracted from the structure adopting different strategies such as calcination at high temperature, supercritical fluid CO_2 (SCF-CO_2) extraction and solvent extraction [22-24]. Although several scientists utilized calcination methods, it fails to guarantee the stability of the structure during the process. The other two approaches, *i.e.* solvent extraction and modified SCF-CO_2, were also utilized before [25, 26]. Solvent extraction method requires a large amount of liquid solvent and a long residence time due to its particular operating condition. On the other hand, Supercritical carbon dioxide is a non-toxic, recyclable and inexpensive solvent which improves the process of template removal. Therefore, we used solvent extraction method combined with modified SCF-CO_2 extraction to decrease the solvent consumption and residence time as well as enhance the surface area of the structure [22, 25]. To the best of Authors knowledge, the combination of both solvent extraction and SCF-CO_2 methods under optimized conditions has not been examined yet.

In this paper, we aim to offer a novel method to improve the extraction efficiency of cationic surfactant from the structure and achieve effective framework with high surface area. Since the magnetic mesoporous silica indicates a slight adsorption capacity, functionalization of this structure is so crucial [27-30]. To serve this goal, scientists proposed numerous types of modification methods such as amino and thiol-functionalized structure, which exhibited a high complexation tendency for the adsorption of Pb^{2+}, Zn^{2+}, Ni^{2+}, Cd^{2+} and Cu^{2+} [31-35]. Therefore, Fe_3O_4@SiO_2@*m*-SiO_2–NH_2 micro-spheres were synthesized by combining both solvent extraction and modified SCF-CO_2 methods to increase the removal of CTAB and reach an efficient adsorbent with significant surface area, which can improve the grafting of amino-groups in the pores. The prepared adsorbent recorded higher adsorption capacity to Cd^{2+} compared to previous adsorbents. The impact of key experimental parameters such as contact time, pH and adsorption capacity of the adsorbent on the removal of cadmium from aqueous solution were investigated.

2. Experimental

2.1. General remarks

2.1.1. Materials

Ammonium hydroxide (aqueous ammonia 28%wt), absolute ethanol (EtOH), tetraethyl orthosilicate (TEOS), ferrous chloride tetrahydrate ($FeCl_2 \cdot 4H_2O$), ferric chloride hexahydrate ($FeCl_3 \cdot 6H_2O$), cetyltrimethylammonium bromide (CTAB), cadmium nitrate ($Cd(NO_3)_2$), and toluene were supplied from Merck & Co. Also, (3-Aminopropyl) triethoxysilane (APTES, 99%) was purchased from Across Co. The whole solvents and chemicals used as received without further treatment.

2.1.2. Instrumentation

Field Emission-Scanning Electron Microscope (FE-SEM) (Hitachi 1460, Japan) was utilized to specify the structure and morphology of microspheres. Particle sizing of the microspheres was determined by using a Particle Size Analyzer (PSA) (JAPA Horiba LB 550). Fourier Transform Infrared Spectroscopy (FT-IR) graphs were derived by a Perkin Elmer FT-IR spectrophotometer (USA). The samples were made ready by grounding with KBr and then pressing into a pellet. The magnetization measurements were calculated using a Vibrating-Sample Magnetometer (VSM) device (Kavir Magnet Company, Kashan, Iran). The EDX studies were performed on a SEM device (TESCAN-Vega 3, Czech Republic). A Bruker D8 advance X-ray diffractometer (XRD) with Cu Kα radiation was applied to evaluate the crystalline structure of microspheres. A PHS-1020 analyzer was utilized to measure the N_2 adsorption–desorption isotherms (at 77 K.) The surface area and pore size distribution of microspheres were determined by BET and BJH methods. Atomic absorption spectrophotometer (Shimadzu, AAS-670/G) was used to calculate the concentration of cadmium ions in the samples.

2.2. Preparation of amino-functionalized Fe_3O_4@SiO_2@*m*-SiO_2

The Fe_3O_4@SiO_2@*m*-SiO_2 microspheres were produced following the method explained by Kheshti and Hassanajili [36] with slight modifications in the extraction methods. First, 0.1 g of as-prepared Fe_3O_4@SiO_2 NPs was dissolved in 20 mL deionized water and 30 mL ethanol by ultra-sonication (15 min). Then, 1.5 mL of ammonia, 0.4 g CTAB and 0.4 mL TEOS were added to the mixture. The resultant suspension was stirred (500 rpm) at room temperature for 7 h. The resultant product was magnetically gathered and dried in a vacuum oven. The obtained sample was then re-dispersed in 100 mL ethanol, stirred at 60°C for 9 hours, washed several times and dried in a vacuum oven for 9 hours. After that, the obtained materials have been transferred to the extraction vessel of a supercritical system where liquid CO_2 and methanol was introduced into the vessel (1 mL min^{-1}) for 3 h under ideal conditions of 180 bar and 80 °C to extract the remained surfactant [37]. The samples were washed and dried at vacuum oven for 6 h. After that, 0.1 g of as- synthesized nanoparticles were dissolved in 70 mL toluene by ultra-sonication. In the next step, 3.5 mL of 3-aminopropyl triethoxysilane was added dropwise to the solution while it was refluxed for 24 h at 115 °C. The formed product was magnetically separated and dried in a vacuum oven after washing with ethanol/acetone solution. Fig. 1 shows the schematic of synthesis reactor.

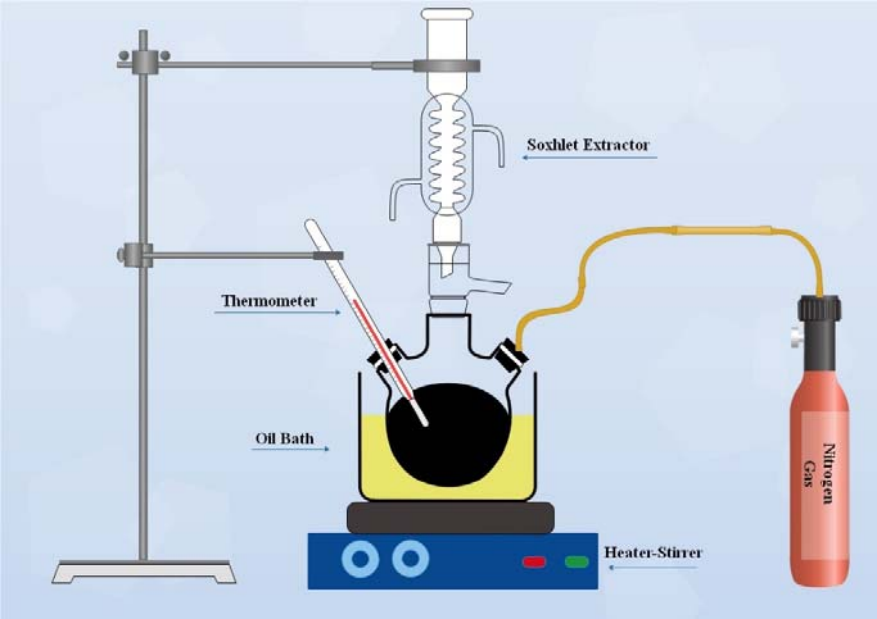

Fig. 1. Schematic of nanoparticle's synthesis reactor

2.3. Adsorption experiments

The cadmium adsorption capability of the prepared sorbent was examined in aqueous solutions containing $Cd(NO_3)_2$. We investigated the removal of cadmium by nano-sorbent in batch experiments at room temperature. 0.5 g of Fe_3O_4@SiO_2@*m*-SiO_2–NH_2 microspheres and 50 mL of Cd^{2+} solution (concentrations of 20-1080 mg L^{-1}) were mixed. After reaching an equilibrium in 60 min, the Fe_3O_4@SiO_2@*m*-SiO_2–NH_2 microspheres were magnetically separated with an external magnet, and the residual concentration of the Cd^{2+} solution was measured. The adsorption experiments were performed three times to ensure the results.

The removal efficiency of Cd can be measured by the following equation:

$$Re\ (\%) = \frac{C_i - C_e}{C_i} \times 100 \qquad (1)$$

Where Re is the removal efficiency of Cd^{2+}, C_i and C_e are the Cd^{2+} concentrations at beginning and equilibrium (mg L^{-1}), respectively.

The adsorption of cadmium was investigated under the following experimental conditions; pH 2 to 8 and contact time 0 to 60 minutes. The equilibrium adsorption capacity for the as-prepared sorbent q_e (mg cadmium per g sorbent) was calculated from equation 2:

$$q_e = (C_i - C_e) \times \frac{V}{m} \qquad (2)$$

where, V and m are the total volume of Cd^{2+} solution (L) and adsorbent mass (g), respectively.

3. Results and discussion

3.1 Fe_3O_4@SiO_2@*m*-SiO_2–NH_2: Preparation and characterization

Fig. 2 shows a schematic diagram of the synthesis of Fe_3O_4@SiO_2@*m*-SiO_2–NH_2 microspheres. As mentioned, the Fe_3O_4@SiO_2 NPs were initially prepared following the methods mentioned in section 2.2. Then, a mesoporous silica shell was coated on the Fe_3O_4@SiO_2 NPs by removing CTAB templates from the structure *via* a combination of solvent extraction and methanol-SCF-CO_2 extraction. Finally, APTES molecules were anchored on the microspheres of Fe_3O_4@SiO_2@*m*-SiO_2 to capture the cadmium ions in the solutions.

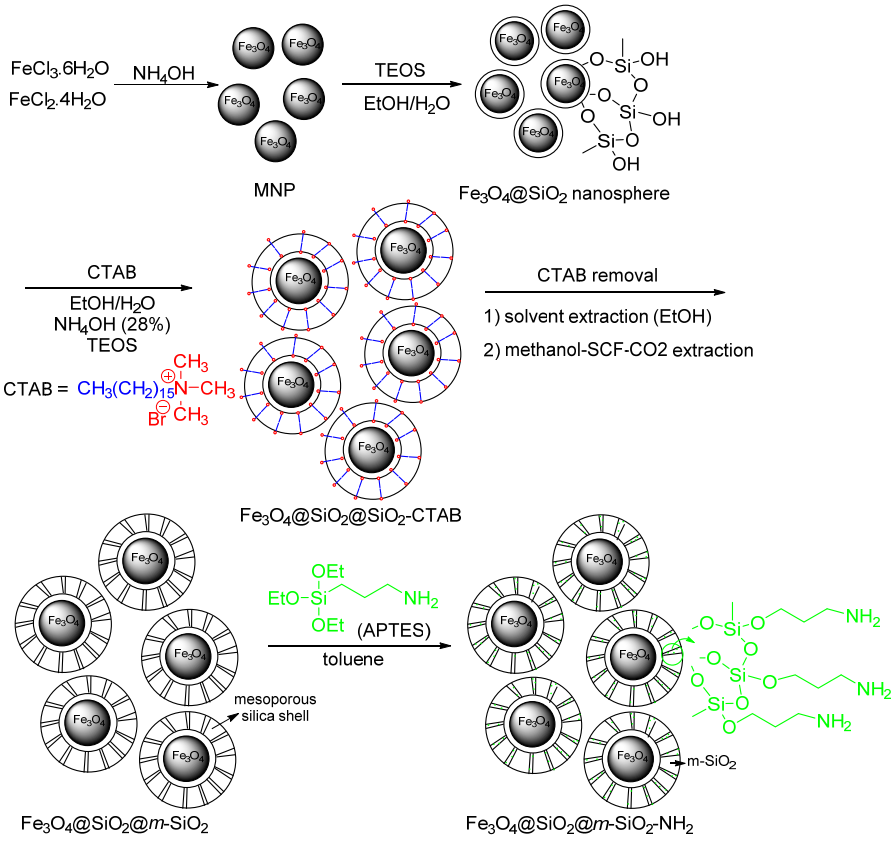

Fig. 2. Schematic of Fe_3O_4@SiO_2@*m*-SiO_2–NH_2 microsphere's synthesis

Fig. 3 represent the FE-SEM and PSA characterization of Fe_3O_4, Fe_3O_4@SiO_2 and Fe_3O_4@SiO_2@*m*-SiO_2–NH_2 microspheres. FE-SEM images shows that the spherical shape of the magnetic core has been unchanged during the coating process and functionalization with 3-aminopropyl triethoxysilane (APTES). The average size of Fe_3O_4, Fe_3O_4@SiO_2 and Fe_3O_4@SiO_2@*m*-SiO_2–NH_2 micro-spheres were 4, 11 and 416 nm, respectively.

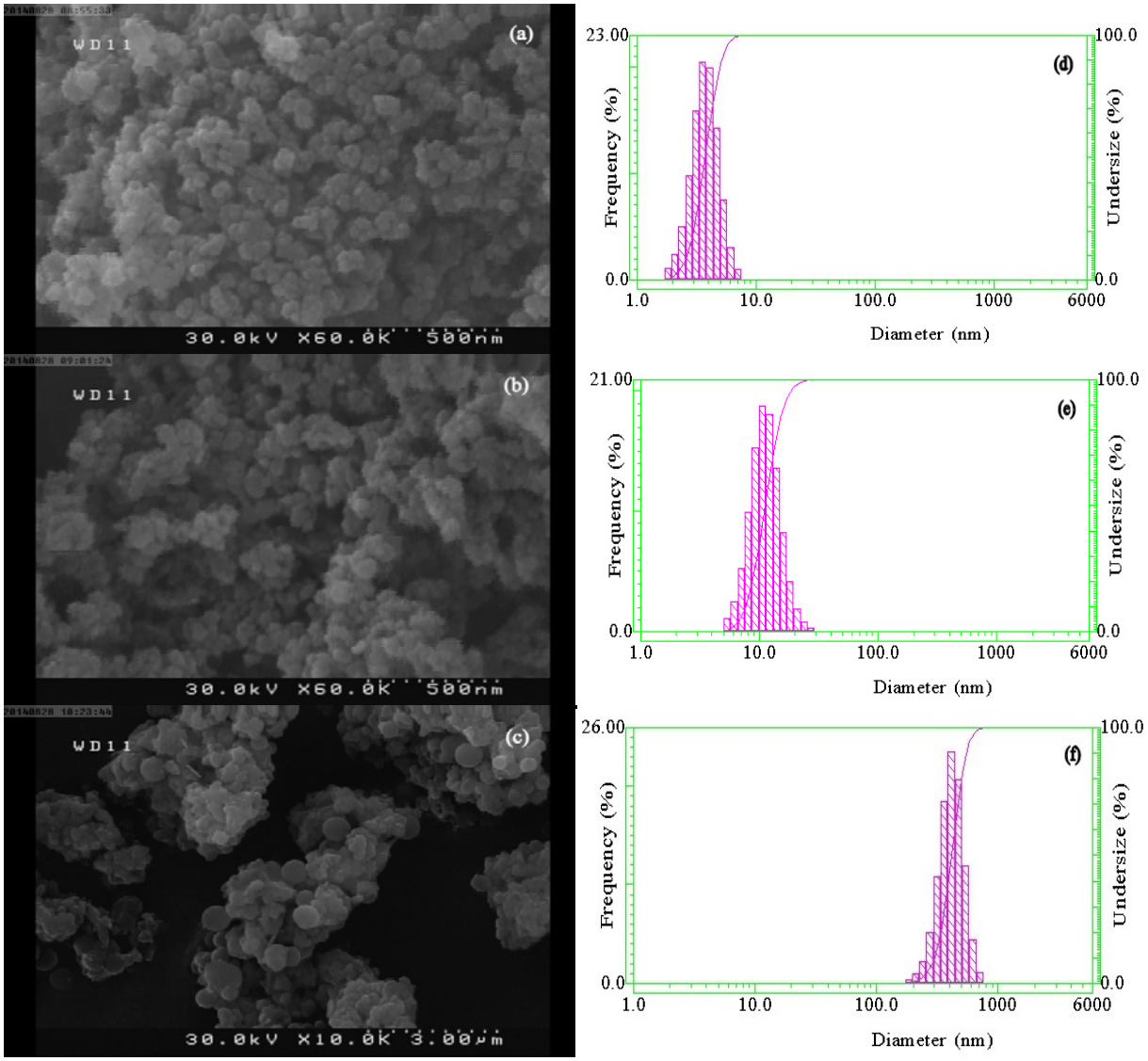

Fig. 3. FE-SEM (a,b,c) and PSA (d,e,f) depictions of Fe_3O_4 (a, d), Fe_3O_4@SiO_2 (b, e) and Fe_3O_4@SiO_2@*m*-SiO_2–NH_2 (c, f)

The FT-IR spectrums of Fe_3O_4, Fe_3O_4@SiO_2, Fe_3O_4@SiO_2@*m*-SiO_2 and Fe_3O_4@SiO_2@*m*-SiO_2–NH_2 microspheres are given in Fig. 4. The peak at 594 cm^{-1} (Fig. 4a) corresponds to Fe-O stretching vibration and confirms that MNP was successfully synthesized. Vibration of symmetric and asymmetric stretching of Si-O-Si bond are recognized at 794 and 1095 cm^{-1} respectively (Fig. 4b) and confirms that silica layer was coated on the magnetic nanoparticles [38]. These peaks can be recognized with a slight shift at 1085 and 794 cm^{-1} for Fe_3O_4@SiO_2@*m*-SiO_2 (Fig. 4c). Furthermore, the broad absorption band at about 3440 cm^{-1} can be corresponded to the stretching vibration of OH group (Fig. 4a-c) [39, 40]. The peaks at 2924 and 2854 cm^{-1} (Fig. 4d) corresponding to –CH_2– groups and the peak at 1460 cm^{-1} (Fig. 4d) is stemmed

from bending vibration of amine groups that verifies the successful grafting of amino group on the Fe_3O_4@SiO_2@*m*-SiO_2 microsphere [41].

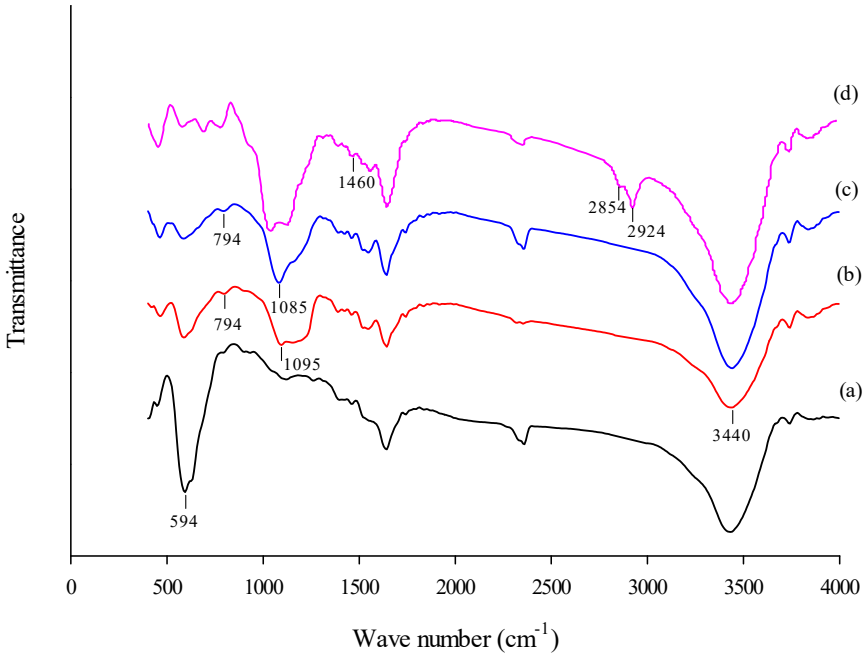

Fig. 4. FT-IR spectra of (a) Fe_3O_4, (b) Fe_3O_4@SiO_2, (c) Fe_3O_4@SiO_2@*m*-SiO_2 and (d) Fe_3O_4@SiO_2@*m*-SiO_2–NH_2

Fig. 5A shows the magnetization diagrams of the Fe_3O_4, Fe_3O_4@SiO_2, and Fe_3O_4@SiO_2@*m*-SiO_2–NH_2 microspheres. The saturation magnetization values of 78, 57 and 30 emu g^{-1} were obtained for Fe_3O_4, Fe_3O_4@SiO_2 and Fe_3O_4@SiO_2@*m*-SiO_2–NH_2, respectively. The decrease in the magnetic saturation value is due to the decrease of the Fe_3O_4 density caused by SiO_2 and *meso*-SiO_2-NH_2 coating [20]. The results reveal that microspheres have strong magnetization, so it can be quickly separated from the solutions by a magnet and re-dispersed rapidly after removing the magnet.

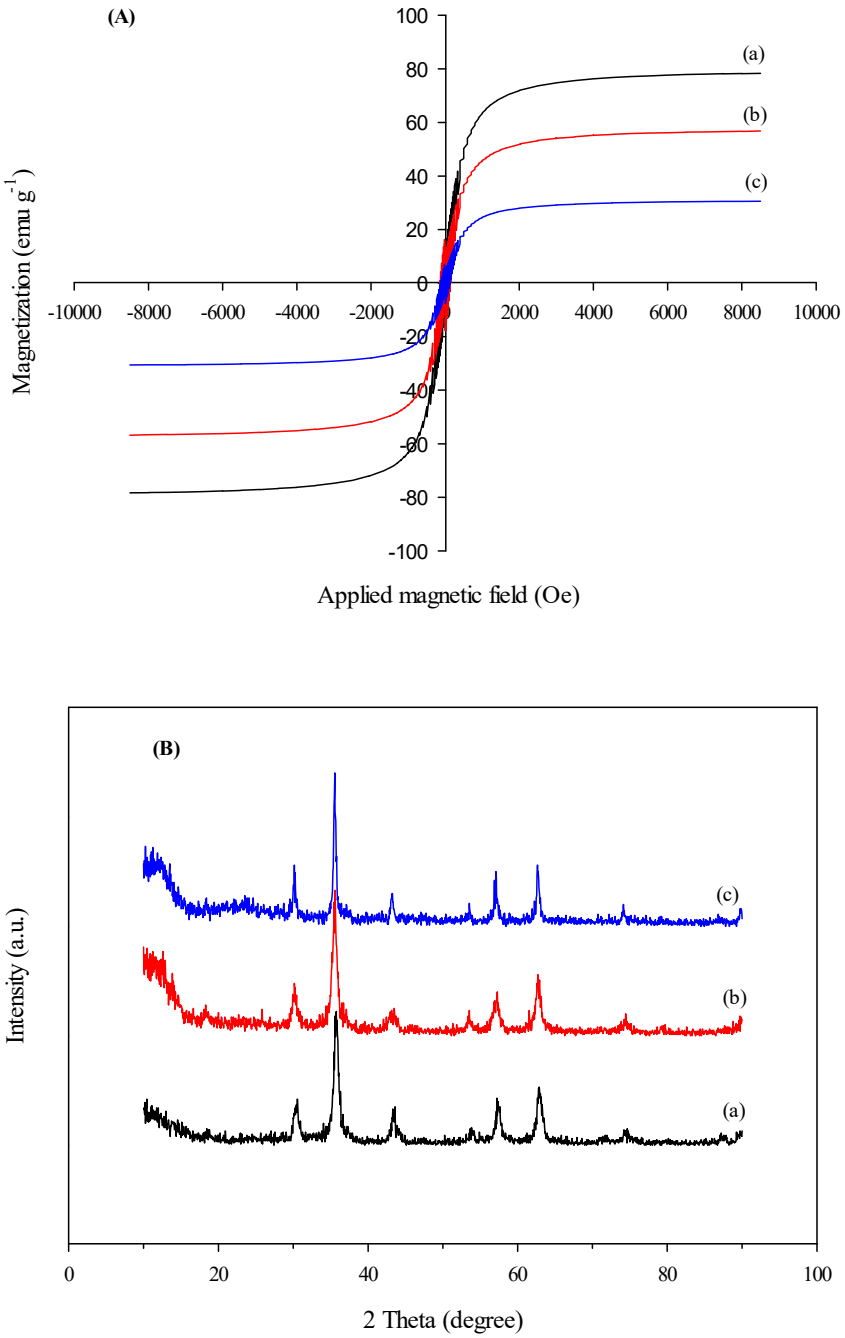

Fig. 5. (A) VSM curves and (B) XRD illustrations of (a) Fe_3O_4, (b) Fe_3O_4@SiO_2 and (c) Fe_3O_4@SiO_2@*m*-SiO_2–NH_2

Fig. 5B shows the XRD analysis of Fe_3O_4, Fe_3O_4@SiO_2, and Fe_3O_4@SiO_2@*m*-SiO_2–NH_2 microspheres. As shown in the Fig. 5B(a), six strong peaks appeared at 2θ = 30.25°, 35.64°, 43.26°, 53.66°, 57.18° and

62.78° are indicated to the face-centered cubic configuration of magnetic NPs [42]. The consistency of these peaks in Fig. 5B(b) and Fig. 5B(c) indicates that the crystalline structure of magnetic NPs through silica coating and amino-functionalization is well maintained. Furthermore, an additional broad peak around 2θ =20° (Fig. 5B(c)) is attributed to the amorphous SiO_2 layer.

The EDX spectrum was applied to recognize the existence of particular elements in the Fe_3O_4@SiO_2@*m*-SiO_2–NH_2 microspheres (Fig. 6). The emission lines of Fe are located at K_α = 6.4, K_β = 7.05 and L_α = 0.70 keV. The peaks located at 0.55, 0.25 and 1.76 keV are related to O, C and Si ions, respectively. This emission lines approved the successful synthesis of Fe_3O_4@SiO_2@*m*-SiO_2 microspheres. Also, the peaks of C (0.3 keV) and N (0.4 keV) are due to ethoxy and amine groups, which indicates the successful grafting of APTES molecules onto the mesoporous structure [43].

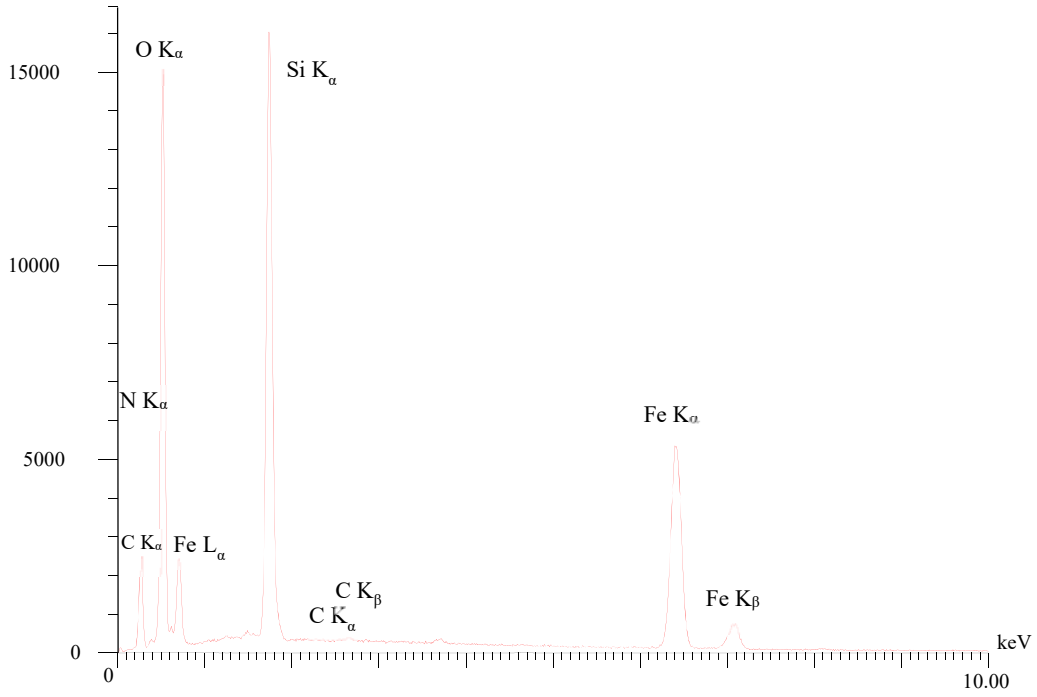

Fig. 6. EDX spectrum of Fe_3O_4@SiO_2@*m*-SiO_2–NH_2 at an acceleration voltage of 10 kV

Fig. 7 shows the isotherms of N_2 adsorption–desorption of magnetic mesoporous silica microspheres before and after amino-functionalization. The mean pore size value of Fe_3O_4@SiO_2@*m*-SiO_2 was 3.46 nm and its total pore volume and BET surface area was calculated as 0.24 cm^3g^{-1} and 867.64 m^2g^{-1}, respectively. After amino-modification, the pore size, total average pore volume, and BET surface area were decreased to 2.85 nm, 0.087 cm^3g^{-1} and 637.38 m^2g^{-1}, respectively. The most probable reason could be the pores blocking of the structure after the amino functionalization process [19]. Table 1 shows that the BET surface area, 637m^2g^{-1}, is larger than that reported in the previous studies, with largest surface area of

503.63 m^2g^{-1} for Amino-functionalized hollow core-mesoporous shell silica. The obtained results indicate the large surface area of the prepared adsorbent, which makes it feasible for the potential applications in the adsorption field.

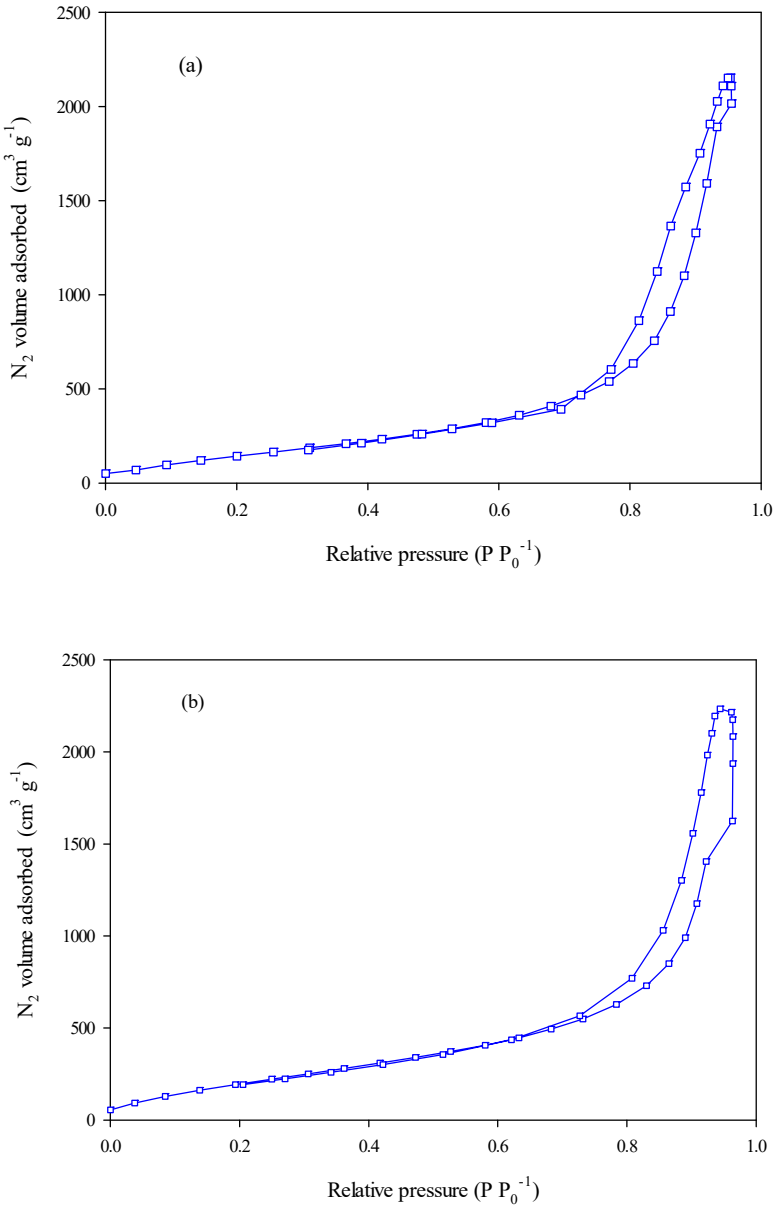

Fig. 7. N_2 adsorption-desorption of (a) Fe_3O_4@SiO_2@*m*-SiO_2 and (b) Fe_3O_4@SiO_2@*m*-SiO_2–NH_2

Table 1. The surface area of prepared adsorbent compared to some adsorbents

Type of adsorbent	Surface area (m^2 g^{-1})	References
Fe_3O_4 sulfonated MNPs	18.32	[18]
Mesoporous silica-calcium phosphate hybrid NPs	314.56	[44]
Granular activated carbon	358.00	[45]
Activated clay	90.00	[45]
Polyacrylamide-modified Fe_3O_4/MnO_2	158.34	[46]
Al_2O_3/carbon composite	358.59	[47]
γ-Fe_2O_3/Fe-doped hydroxyapatite	98.20	[48]
Amino-functionalized hollow core-mesoporous shell silica	503.63	[49]
Fe_3O_4@SiO_2@*m*-SiO_2–NH_2	637.38	This work

3.2 Adsorption experiments

3.2.1. Influence of pH of a solution and contact time on Cd^{2+} ion adsorption

pH is one of the greatest effective variables in cadmium removal process. Typically, 50 mg of synthesized microspheres were mixed with 50 mL of 870 mg L^{-1} Cd^{2+} solution. To adjust the pH of a solution, a range of 2 to 8, drops of HCl or NaOH was added to the samples. These samples were agitated for 60 min and adsorbents were separated after achieving the adsorption equilibrium. The supernatant was analyzed to measure the concentration of cadmium ion.

As illustrated in Fig. 8a, the removal efficiency of Cd^{2+} was significantly increased with increasing the pH from 2-6 but remained fix at pH of 6 or higher. Under acidic pH, the amino groups of the adsorbent are protonated and its binding capacity to Cd^{2+} ions was subsequently decreased. As the solution pH increased to 6, the adsorption capacity of Cd^{2+} by the adsorbent increased noticeably; this is because the free lone pairs of nitrogen atoms in the amino group, which improved the adsorption characteristics of the microspheres. At pH > 6, the amino groups are deprotonated resulting in a constant removal efficiency. Consequently, the optimal solution pH is considered to be pH 6.

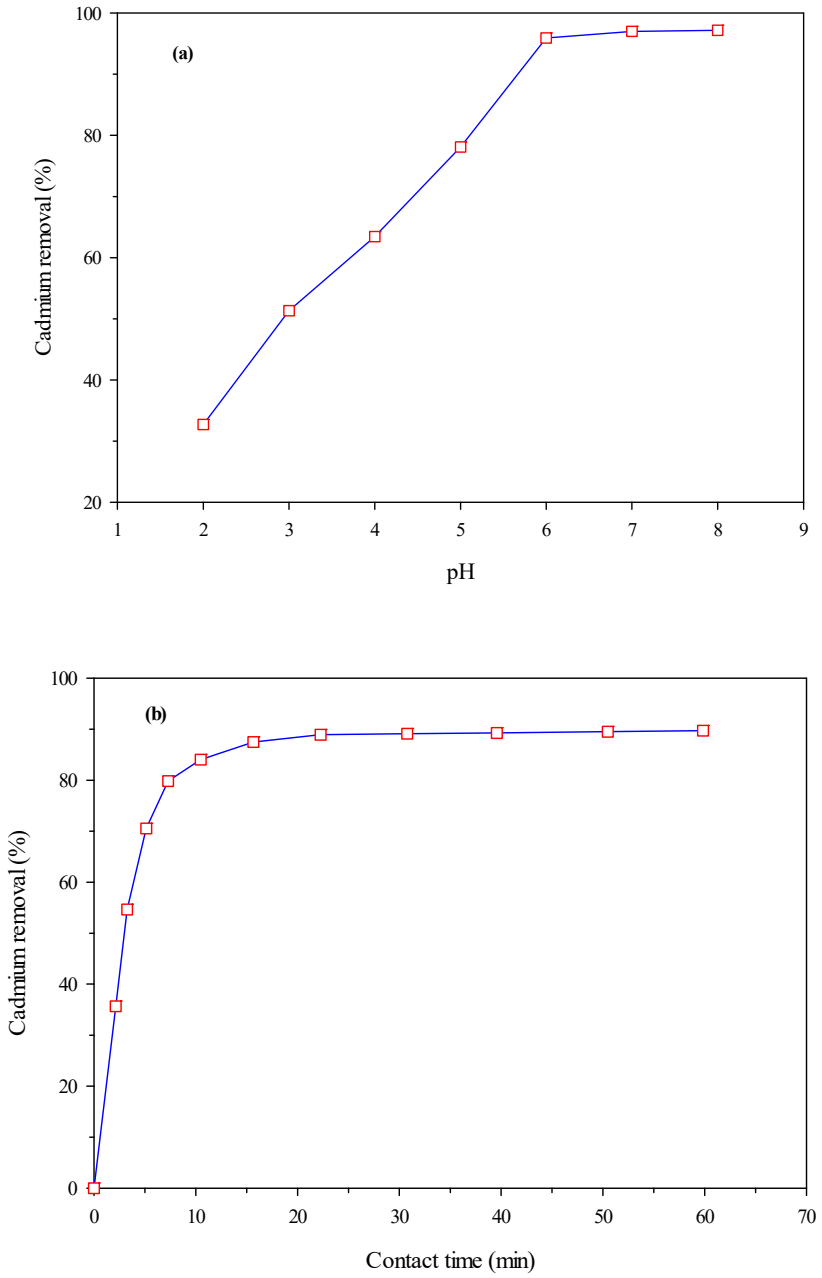

Fig. 8. Effect of (a) pH and (b) contact time on Cd^{2+} removal (adsorbent amount: 50 mg, volume of Cd^{2+}solution: 50 mL, primary concentration of cadmium: 870 mg L^{-1}, T= 298 K).

To study the impact of contact time on the adsorption of Cd^{2+}, kinetics experiments were performed by mixing 50 mg of the sorbent with 50 mL Cd^{2+} solution (initial concentration = 870 mg L^{-1}) at an optimum pH-value of 6. The solution has been stirred from 0 to 60 min and the concentration of Cd^{2+} was measured by Atomic Absorption Spectrophotometer (AAS).

Fig. 8b illustrates that the Cd^{2+} adsorption equilibrium was almost achieved during the first 20 min. During the first 10 minutes, more than 90% of Cd^{2+} was removed. Then, the removal efficiency almost leveled out at 20 minutes and did not improve significantly to the end of test after 60 min. This behavior was due to the availability of many active sites at the beginning of cadmium removal process, which occupied over time and cadmium adsorption reduced. A contact time of 60 min was selected in subsequent experiments to ensure the equilibrium adsorption.

3.2.2 Adsorption kinetics

The pseudo-first-order, pseudo-second-order and intra-particle diffusion models were applied to analyze the cadmium adsorption rate and realize the adsorption kinetics (Fig. 9). The linearized pseudo-first-order kinetic model is [50]:

$$\ln (q_e - q_t) = \ln q_e - k_1 t \quad (3)$$

The pseudo-second-order model is linearly demonstrated as given in Equation 4 [51]:

$$\frac{t}{q_t} = \frac{1}{k_2 q_e^2} + \frac{t}{q_e} \quad (4)$$

Where, q_e is the adsorbed Cd^{2+} (mg g^{-1}) at equilibrium, q_t is the adsorbed Cd^{2+} (mg g^{-1}) at time t (min), k_1 is pseudo-first-order rate constant (min^{-1}) and k_2 is pseudo-second-order rate constant (g $mg^{-1}min^{-1}$).

Table 2 shows the obtained parameters for the mentioned models. As seen, the correlation coefficient (R^2) of the second kinetic is almost equal to 1, indicating that the sorption kinetic follows the pseudo-second-order model and the chemical adsorption of Cd^{2+} ions onto the adsorbent is a rate-controlling step [51]. In addition, the equilibrium adsorption capacity obtained from the experimental data ($q_{e,exp}$ = 834.2 mg g^{-1}) is close to the estimated value for the pseudo-second-order kinetic.

Also, the intra-particle diffusion model was applied to interpret the kinetic data by using the Weber-Morris equation as [52]:

$$q_t = k_{id}\, t^{0.5} + C \quad (5)$$

where, k_{id} is rate constant (mg g^{-1} $min^{-0.5}$) and C is the intercept (mg g^{-1}).

As illustrated in Fig. 9c, the plot of q_t versus $t^{0.5}$ has two different adsorption stages. The initial (linear) stage could be related to rapid surface adsorption and intra-particle diffusion. The second (plateau) stage, where the intra-particle diffusion begins to decelerate, can be ascribed to the pore diffusion [53].

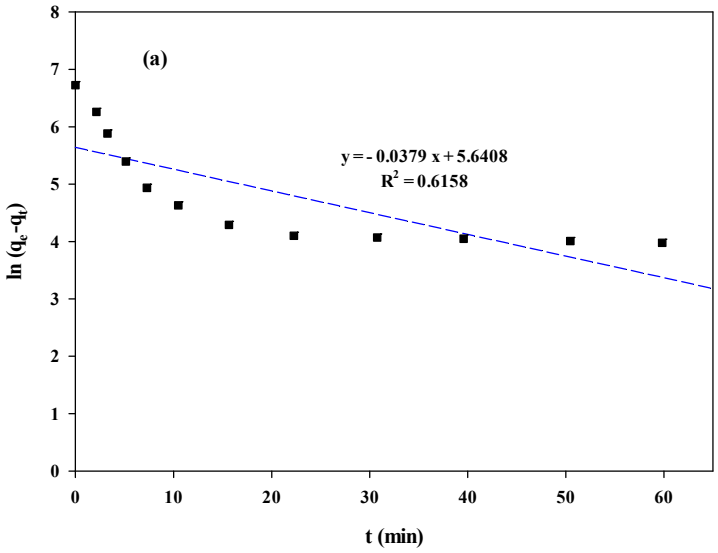

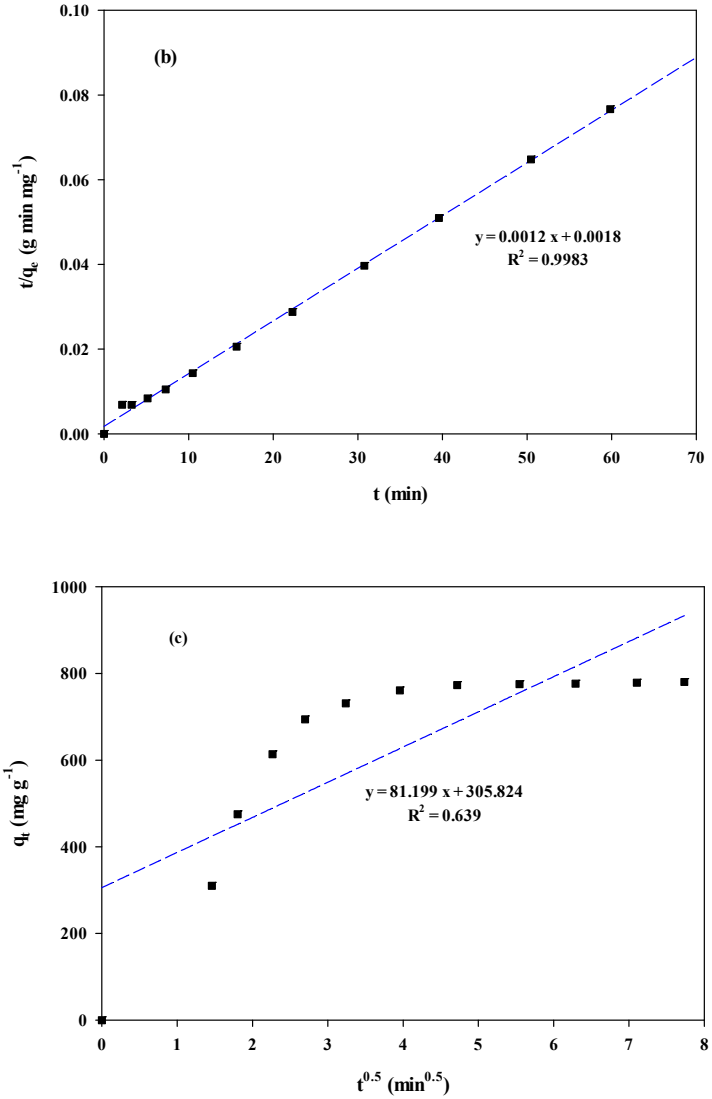

Fig. 9. Pseudo-first-order (a), pseudo-second-order (b), and Intra-particle diffusion (c) fit of Cd^{2+} adsorption on Fe_3O_4@SiO_2@*m*-SiO_2–NH_2 (Adsorbent dose: 50 mg, Cd^{2+} concentration: 870 mg L^{-1}, solution volume: 50 mL, pH= 6, T= 298 K)

Table 2. Calculated parameters for adsorption kinetic models.

Pseudo-first-order			Pseudo-second-order			Intra-particle diffusion		
$q_{e,cal}$ (mg g^{-1})	k_1 (min^{-1})	R^2	$q_{e,cal}$ (mg g^{-1})	k_2 (g $mg^{-1}min^{-1}$)	R^2	k_{id} (mg g^{-1} $min^{-0.5}$)	C (mg g^{-1})	R^2
281.68	0.038	0.616	833.33	0.0008	0.998	81.19	305.82	0.64

3.2.3 Adsorption Isotherms and reusability

Fig. 10 indicates the equilibrium adsorption capacity of microspheres (q_e) versus the equilibrium concentration of Cd^{2+} (C_e). Apparently, the adsorption capacity of adsorbent gradually increases by enhancing the equilibrium concentration of Cd^{2+} ion to reach a maximum level of 834.2 mg g^{-1} and then kept almost unchanged. A comparison between the adsorption capacity in this study and adsorbents in previous studies is shown in Table 3. The maximum adsorption capacity in this work is 2 to 28 times greater than previously developed adsorbents [15, 18, 19, 46, 54-57]. This is due to an enormous amount of free amino-grafted mesoporous sites inside the Fe_3O_4@SiO_2@*m*-SiO_2–NH_2 structure. Therefore, the prepared microsphere through a combination of solvent extraction and methanol-SCF-CO_2 extraction followed by amino-functionalization is a proper adsorbent for the removal of cadmium ions.

The Langmuir, Freundlich, and Temkin isotherms were fitted to experimental data to interpret the adsorption (Fig. 10). The Langmuir isotherm presumes that the adsorption of adsorbate on the sorbent is monolayer and can be defined as follows [58, 59]:

$$q_e = \frac{q_m k_L C_e}{1+k_L C_e} \quad (6)$$

where, q_m is maximum capacity of monolayer coverage (mg g^{-1}), k_L is isotherm constant attributed to the adsorption energy (L mg^{-1}).

The Freundlich isotherm, which assumes that multi-layer adsorption happens through heterogeneous adsorption system is shown as follows [60, 61]:

$$q_e = k_f C_e^{\ 1/n} \quad (7)$$

where, k_f is Freundlich adsorption constant (mg g^{-1}) and n is an empirical parameter due to adsorption intensity. The calculated constants for these isotherms are tabulated in Table 4. As shown in Table 4, the Langmuir isotherm fitted very well with the kinetic data (R^2>0.99). As such, adsorption of cadmium ions on the surface of sorbent is restricted to monolayer coverage.

Furthermore, the experimental data were assessed with Temkin isotherm. This isotherm deals with adsorbent-adsorbate interactions and presumes that the adsorption heat of molecules linearly reduces with surface coverage [62, 63]. The Temkin isotherm can be described as:

$$q_e = \frac{RT}{b_T} \mathrm{Ln}(A_T C_e) \quad (8)$$

where, $B=\frac{RT}{b_T}$ is isotherm constant associated with adsorption heat (J mol^{-1}), A_T is equilibrium binding constant regarding the binding energy of maximum (L mg^{-1}), R is gas constant (8.3 J mol^{-1} K^{-1}), T is absolute temperature (K). Table 4 shows the obtained constants for this model, which indicates that the distribution of binding energies is unequal and adsorption reaction is exothermic (B > 0) [53, 64].

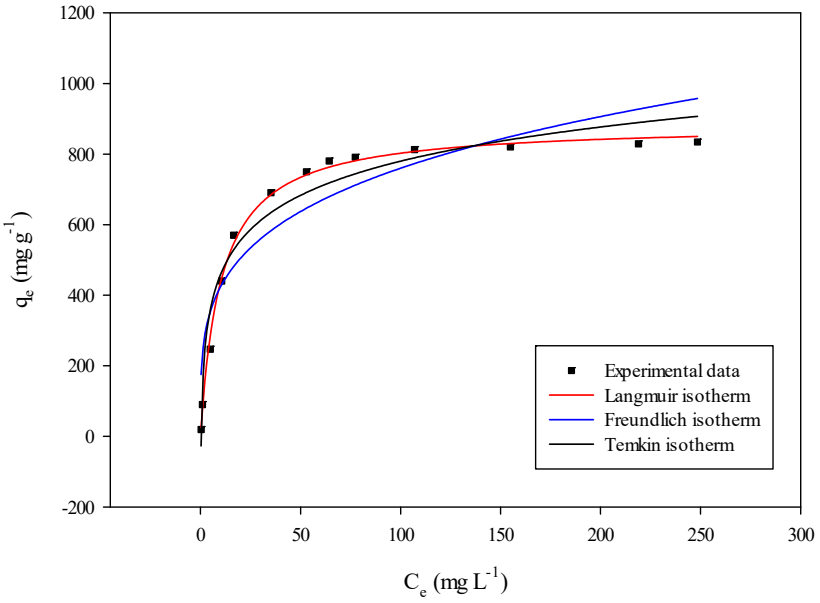

Fig. 10. Equilibrium adsorption isotherms of Fe_3O_4@SiO_2@*m*-SiO_2–NH_2 toward Cd^{2+} from aqueous solution (Adsorbent dose: 50 mg, Cd^{2+} concentrations: 20-843 mg L^{-1}, solution volume: 50 mL, pH= 6, contact time: 60 min, T= 298 K)

Table 3. The adsorption capacity of Fe_3O_4@SiO_2@*m*-SiO_2–NH_2 compared to some adsorbents

Type of adsorbent	Adsorption capacity (mg g^{-1})	References
Fe_3O_4/APS/AA-co-CA	29.60	[15]
Fe_3O_4 sulfonated magnetic NP	80.90	[18]
Fe_3O_4@SiO_2@*meso*-SiO_2–NH_2	492.40	[19]
Polyacrylamide-modified Fe_3O_4/MnO_2	39.05	[46]
Amino functional mesoporous silica SBA-15	93.30	[54]
Magnetic functionalized MCM-48 mesoporous silica	114.08	[55]
Nanoscale zero-valent iron (nZVI)	66.90	[56]
Amino-functionalized Fe_3O_4@mesoporous SiO_2	51.80	[57]
Fe_3O_4@SiO_2@*m*-SiO_2–NH_2	834.18	This work

Table 4. Langmuir, Freundlich and Temkin isotherms parameters

Langmuir isotherm			Freundlich isotherm			Temkin isotherm		
q_m (mg g^{-1})	k_L (L mg^{-1})	R^2	n	k_f (mg g^{-1})	R^2	b_T	A_T (L mg^{-1})	R^2
884.906	86.1014	0.9967	3.9385	236.031	0.8755	17.7438	2.6673	0.9604

To confirm the feasibility of recycling and reuse of saturated Fe_3O_4@SiO_2@*m*-SiO_2–NH_2 microspheres, HCl solution (1 M) was added to the saturated Fe_3O_4@SiO_2@m-SiO_2–NH_2 and mix for 1 h. As shown in Fig. 11, the adsorption capacity of adsorbent kept approximately unchanged after 6 cycles, which shows that the synthesized microsphere possesses exceptional reusability and chemical stability. Cadmium removal was 92% after 6 cycles by regeneration with strong acid solution. This will reduce the treatment cost of contaminated water by magnetic nanoparticles while cadmium ions can be recovered from solution by chemical reactions. In general, the study showed promising results of using mesoporous silica for the removal of Cd2+ from aqueous solution. This technique can be practically used in the removal of such waste on from contaminated wastewaters where other technologies suffer technical problems such as membrane fouling or low removal efficiency.

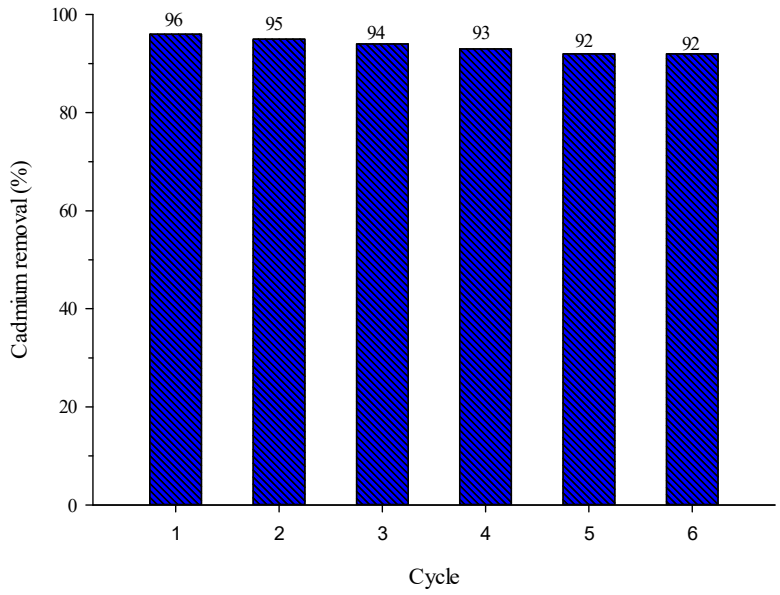

Fig. 11. Effect of different cycles in the removal efficiency of the adsorbent (adsorbent: 50 mg, recovery solution: 1 M HCl, mixing time: 1 h, and temperature: 298 K)

4. Conclusion

A novel mesoporous microsphere with a core-shell structure was produced in laboratory for the removal of cadmium from solution. This structure formed from a magnetic Fe_3O_4 core, a dense layer of silica, and a mesoporous shell of amino-functionalized silica. Adopting unique methodology based on the combination of modified SCF-CO_2 and solvent extraction to remove the template from structure offered amino-modified magnetic mesoporous silica with great surface area (637.383 $m^2\ g^{-1}$). The adsorbent was characterized by FE-SEM, FT-IR, VSM, XRD, EDX and N_2 adsorption-desorption analysis which proved that amino-functionalized magnetic mesoporous silica microsphere was successfully synthesized. The prepared adsorbent demonstrated high capability for the removal of Cd^{2+} ions from aqueous solutions. The adsorption of cadmium reached equilibrium at pH 6 and with a contact time equal 60 min. The developed adsorbent has a maximum adsorption capacity equal to 884.906 mg g^{-1}, which is superior to the previously reported adsorption capacity. Furthermore, the kinetic data were in agreement with Langmuir isotherm and the pseudo-second-order models. Cadmium ion can be desorbed by 1 M HCl solution and the regenerated Fe_3O_4@SiO_2@*m*-SiO_2–NH_2 microspheres could retain the original capacity for metal removal.

References

[1] J. Wang and C. Chen, "Biosorbents for heavy metals removal and their future," *Biotechnology advances,* vol. 27, pp. 195-226, 2009.

[2] A. Azimi, A. Azari, M. Rezakazemi, and M. Ansarpour, "Removal of heavy metals from industrial wastewaters: a review," *ChemBioEng Reviews,* vol. 4, pp. 37-59, 2017.

[3] Y. Huang, X. Zeng, L. Guo, J. Lan, L. Zhang, and D. Cao, "Heavy metal ion removal of wastewater by zeolite-imidazolate frameworks," *Separation and Purification Technology,* vol. 194, pp. 462-469, 2018.

[4] R. Ahmad and A. Mirza, "Facile one pot green synthesis of Chitosan-Iron oxide (CS-Fe_2O_3) nanocomposite: Removal of Pb (II) and Cd (II) from synthetic and industrial wastewater," *Journal of Cleaner Production,* vol. 186, pp. 342-352, 2018.

[5] E. J. Tokar, L. Benbrahim-Tallaa, and M. P. Waalkes, "Metal ions in human cancer development," *Metal Ions in Toxicology: Effects, Interactions, Interdependencies,* vol. 8, p. 375, 2015.

[6] C. de Angelis, M. Galdiero, C. Pivonello, C. Salzano, D. Gianfrilli, P. Piscitelli, *et al.*, "The environment and male reproduction: the effect of cadmium exposure on reproductive system and semen quality and its implication in fertility," *Reproductive Toxicology,* 2017.

[7] W. Chansuvarn, Y. Pandee, A. Saechim, and K. Habunmee, "Adsorption of Cadmium (II) Ion from Aqueous Solution onto a Raw Material of Bamboo Powder and its Surface Modification," in *Applied Mechanics and Materials*, 2018, pp. 131-136.

[8] J. E. Efome, D. Rana, T. Matsuura, and C. Q. Lan, "Experiment and modeling for flux and permeate concentration of heavy metal ion in adsorptive membrane filtration using a metal-organic framework incorporated nanofibrous membrane," *Chemical Engineering Journal,* vol. 352, pp. 737-744, 2018.

[9] X. Hou, H. Zhou, J. Zhang, Y. Cai, F. Huang, and Q. Wei, "High Adsorption Pearl-Necklace-Like Composite Membrane Based on Metal–Organic Framework for Heavy Metal Ion Removal," *Particle & Particle Systems Characterization,* p. 1700438, 2018.

[10] J. Ma, Y. He, G. Zeng, F. Li, Y. Li, J. Xiao, *et al.*, "Bio-inspired method to fabricate poly-dopamine/reduced graphene oxide composite membranes for dyes and heavy metal ion removal," *Polymers for Advanced Technologies,* vol. 29, pp. 941-950, 2018.

[11] G. Zhou, J. Luo, C. Liu, L. Chu, and J. Crittenden, "Efficient heavy metal removal from industrial melting effluent using fixed-bed process based on porous hydrogel adsorbents," *Water research,* vol. 131, pp. 246-254, 2018.

[12] G. Crini, "Non-conventional low-cost adsorbents for dye removal: a review," *Bioresource technology,* vol. 97, pp. 1061-1085, 2006.

[13] H. Yaacoubi, O. Zidani, M. Mouflih, M. Gourai, and S. Sebti, "Removal of cadmium from water using natural phosphate as adsorbent," *Procedia engineering,* vol. 83, pp. 386-393, 2014.

[14] L. Khezamia, K. K. Tahaa, E. Amamic, I. Ghiloufid, and L. El Mird, "Removal of Cadmium (II) from aqueous solution by zinc oxide nanoparticles: kinetic and thermodynamic studies," *Desalination and Water Treatment,* vol. 62, pp. 346-354, 2017.

[15] F. Ge, M.-M. Li, H. Ye, and B.-X. Zhao, "Effective removal of heavy metal ions Cd^{2+}, Zn^{2+}, Pb^{2+}, Cu^{2+} from aqueous solution by polymer-modified magnetic nanoparticles," *Journal of hazardous materials,* vol. 211, pp. 366-372, 2012.

[16] M. Khiadani, M. Foroughi, and M. M. Amin, "Improving urban run-off quality using iron oxide nanoparticles with magnetic field," *Desalination and Water Treatment,* vol. 52, pp. 678-682, 2014.

[17] H. Zhang, Z. Zhao, X. Xu, and L. Li, "Study on industrial wastewater treatment using superconducting magnetic separation," *Cryogenics,* vol. 51, pp. 225-228, 2011.

[18] K. Chen, J. He, Y. Li, X. Cai, K. Zhang, T. Liu, *et al.*, "Removal of cadmium and lead ions from water by sulfonated magnetic nanoparticle adsorbents," *Journal of colloid and interface science,* vol. 494, pp. 307-316, 2017.

[19] Q. Yuan, N. Li, Y. Chi, W. Geng, W. Yan, Y. Zhao, *et al.*, "Effect of large pore size of multifunctional mesoporous microsphere on removal of heavy metal ions," *Journal of hazardous materials,* vol. 254, pp. 157-165, 2013.

[20] W. Li, B. Zhang, X. Li, H. Zhang, and Q. Zhang, "Preparation and characterization of novel immobilized Fe_3O_4@ SiO_2@ $mSiO_2$–Pd (0) catalyst with large pore-size mesoporous for Suzuki coupling reaction," *Applied Catalysis A: General,* vol. 459, pp. 65-72, 2013.

[21] B. Min and M. Wenzhong, "Study on core–shell–shell structured nanoparticles with magnetic and luminescent features: Construction, characterization and oxygen-sensing behavior," *Journal of Luminescence,* vol. 141, pp. 80-86, 2013.

[22] Z. Huang, L. Xu, and J.-H. Li, "Amine extraction from hexagonal mesoporous silica materials by means of methanol-enhanced supercritical CO_2: Experimental and modeling," *Chemical engineering journal,* vol. 166, pp. 461-467, 2011.

[23] Z. Huang, J.-h. Li, H. s. Li, H. Miao, S. Kawi, and A. Goh, "Effect of the polar modifiers on supercritical extraction efficiency for template removal from hexagonal mesoporous silica materials: solubility parameter and polarity considerations," *Separation and Purification Technology,* vol. 118, pp. 120-126, 2013.

[24] Z. Huang, J.-h. Li, H.-s. Li, L.-j. Teng, S. Kawi, and M. Lai, "Effects of polar modifiers on supercritical extraction efficiency for organic template removal from mesoporous MCM-41 materials," *The Journal of Supercritical Fluids,* vol. 82, pp. 96-105, 2013.

[25] Z. Huang, H.-s. Li, H. Miao, Y.-h. Guo, and L.-j. Teng, "Modified supercritical CO_2 extraction of amine template from hexagonal mesoporous silica (HMS) materials: effects of template identity and matrix Al/Si molar ratio," *Chemical Engineering Research and Design,* vol. 92, pp. 1371-1380, 2014.

[26] L. Zhao, Y. Chi, Q. Yuan, N. Li, W. Yan, and X. Li, "Phosphotungstic acid anchored to amino–functionalized core–shell magnetic mesoporous silica microspheres: A magnetically recoverable

nanocomposite with enhanced photocatalytic activity," *Journal of colloid and interface science,* vol. 390, pp. 70-77, 2013.

[27] X. Zhuang, Q. Zhao, and Y. Wan, "Multi-constituent co-assembling ordered mesoporous thiol-functionalized hybrid materials: synthesis and adsorption properties," *Journal of Materials Chemistry,* vol. 20, pp. 4715-4724, 2010.

[28] M. Thirumavalavan, Y.-T. Wang, L.-C. Lin, and J.-F. Lee, "Monitoring of the structure of mesoporous silica materials tailored using different organic templates and their effect on the adsorption of heavy metal ions," *The Journal of Physical Chemistry C,* vol. 115, pp. 8165-8174, 2011.

[29] J. Huang, M. Ye, Y. Qu, L. Chu, R. Chen, Q. He, *et al.*, "Pb (II) removal from aqueous media by EDTA-modified mesoporous silica SBA-15," *Journal of colloid and interface science,* vol. 385, pp. 137-146, 2012.

[30] C. McManamon, A. M. Burke, J. D. Holmes, and M. A. Morris, "Amine-functionalised SBA-15 of tailored pore size for heavy metal adsorption," *Journal of colloid and interface science,* vol. 369, pp. 330-337, 2012.

[31] T. Yokoi, Y. Kubota, and T. Tatsumi, "Amino-functionalized mesoporous silica as base catalyst and adsorbent," *Applied Catalysis A: General,* vol. 421, pp. 14-37, 2012.

[32] M. Machida, B. Fotoohi, Y. Amamo, T. Ohba, H. Kanoh, and L. Mercier, "Cadmium (II) adsorption using functional mesoporous silica and activated carbon," *Journal of hazardous materials,* vol. 221, pp. 220-227, 2012.

[33] X. Xin, Q. Wei, J. Yang, L. Yan, R. Feng, G. Chen, *et al.*, "Highly efficient removal of heavy metal ions by amine-functionalized mesoporous Fe_3O_4 nanoparticles," *Chemical Engineering Journal,* vol. 184, pp. 132-140, 2012.

[34] G. Li, Z. Zhao, J. Liu, and G. Jiang, "Effective heavy metal removal from aqueous systems by thiol functionalized magnetic mesoporous silica," *Journal of hazardous materials,* vol. 192, pp. 277-283, 2011.

[35] H. Zheng, D. Hu, L. Zhang, and T. Rufford, "Thiol functionalized mesoporous silicas for selective adsorption of precious metals," *Minerals Engineering,* vol. 35, pp. 20-26, 2012.

[36] Z. Kheshti and S. Hassanajili, "Novel Multifunctional Mesoporous Microsphere with High Surface Area for Removal of Zinc Ion from Aqueous Solution: Preparation and Characterization," *Journal of Inorganic and Organometallic Polymers and Materials,* vol. 27, pp. 1613-1626, 2017.

[37] Z. Kheshti and S. Hassanajili, "Surfactant Removal from Mesoporous Silica Shell of Core-Shell Magnetic Microspheres by Modified Supercritical CO_2," *International Journal of Nanoscience and Nanotechnology,* vol. 13, pp. 119-127, 2017.

[38] Z. Xu, Y. Feng, X. Liu, M. Guan, C. Zhao, and H. Zhang, "Synthesis and characterization of Fe_3O_4@ SiO_2@ poly-l-alanine, peptide brush–magnetic microspheres through NCA chemistry for drug delivery and enrichment of BSA," *Colloids and Surfaces B: Biointerfaces,* vol. 81, pp. 503-507, 2010.

[39] L. Wang, Y. Sun, J. Wang, J. Wang, A. Yu, H. Zhang, *et al.*, "Preparation of surface plasmon resonance biosensor based on magnetic core/shell Fe_3O_4/SiO_2 and $Fe_3O_4/Ag/SiO_2$ nanoparticles," *Colloids and Surfaces B: Biointerfaces,* vol. 84, pp. 484-490, 2011.

[40] S. N. Abdollahi, M. Naderi, and G. Amoabediny, "Synthesis and physicochemical characterization of tunable silica–gold nanoshells via seed growth method," *Colloids and Surfaces A: Physicochemical and Engineering Aspects,* vol. 414, pp. 345-351, 2012.

[41] J. Wang, S. Zheng, Y. Shao, J. Liu, Z. Xu, and D. Zhu, "Amino-functionalized Fe_3O_4@ SiO_2 core–shell magnetic nanomaterial as a novel adsorbent for aqueous heavy metals removal," *Journal of Colloid and Interface Science,* vol. 349, pp. 293-299, 2010.

[42] X. Zhang, H. Niu, Y. Pan, Y. Shi, and Y. Cai, "Modifying the surface of Fe_3O_4/SiO_2 magnetic nanoparticles with C_{18}/NH_2 mixed group to get an efficient sorbent for anionic organic pollutants," *Journal of colloid and interface science,* vol. 362, pp. 107-112, 2011.

[43] S. H. Araghi, M. H. Entezari, and M. Chamsaz, "Modification of mesoporous silica magnetite nanoparticles by 3-aminopropyltriethoxysilane for the removal of Cr (VI) from aqueous solution," *Microporous and Mesoporous Materials,* vol. 218, pp. 101-111, 2015.

[44] Y. He, L. Luo, S. Liang, M. Long, and H. Xu, "Synthesis of mesoporous silica-calcium phosphate hybrid nanoparticles and their potential as efficient adsorbent for cadmium ions removal from aqueous solution," *Journal of Colloid and Interface Science,* vol. 525, pp. 126-135, 2018.

[45] K. L. Wasewar, P. Kumar, S. Chand, B. N. Padmini, and T. T. Teng, "Adsorption of cadmium ions from aqueous solution using granular activated carbon and activated clay," *CLEAN–Soil, Air, Water,* vol. 38, pp. 649-656, 2010.

[46] Z. Liu, X. Li, P. Zhan, F. Hu, and X. Ye, "Removal of cadmium and copper from water by a magnetic adsorbent of PFM: Adsorption performance and micro-structural morphology," *Separation and Purification Technology,* 2018.

[47] H. Chen, J. Luo, X. Wang, X. Liang, Y. Zhao, C. Yang, *et al.*, "Synthesis of Al_2O_3/carbon composites from wastewater as superior adsorbents for Pb (II) and Cd (II) removal," *Microporous and Mesoporous Materials,* vol. 255, pp. 69-75, 2018.

[48] X. Xiao, L. Yang, D. Zhou, J. Zhou, Y. Tian, C. Song, *et al.*, "Magnetic γ-Fe_2O_3/Fe-doped hydroxyapatite nanostructures as high-efficiency cadmium adsorbents," *Colloids and Surfaces A: Physicochemical and Engineering Aspects,* vol. 555, pp. 548-557, 2018.

[49] A. M. El-Toni, M. A. Habila, M. A. Ibrahim, J. P. Labis, and Z. A. ALOthman, "Simple and facile synthesis of amino functionalized hollow core–mesoporous shell silica spheres using anionic surfactant for Pb (II), Cd (II), and Zn (II) adsorption and recovery," *Chemical Engineering Journal,* vol. 251, pp. 441-451, 2014.

[50] Y.-M. Hao, C. Man, and Z.-B. Hu, "Effective removal of Cu (II) ions from aqueous solution by amino-functionalized magnetic nanoparticles," *Journal of Hazardous Materials,* vol. 184, pp. 392-399, 2010/12/15/ 2010.

[51] M. Monier, D. M. Ayad, Y. Wei, and A. A. Sarhan, "Adsorption of Cu(II), Co(II), and Ni(II) ions by modified magnetic chitosan chelating resin," *Journal of Hazardous Materials,* vol. 177, pp. 962-970, 2010/05/15/ 2010.

[52] W. J. Weber and J. C. Morris, "Kinetics of adsorption on carbon from solution," *Journal of the Sanitary Engineering Division,* vol. 89, pp. 31-60, 1963.

[53] M. Kousha, E. Daneshvar, M. S. Sohrabi, M. Jokar, and A. Bhatnagar, "Adsorption of acid orange II dye by raw and chemically modified brown macroalga Stoechospermum marginatum," *Chemical Engineering Journal,* vol. 192, pp. 67-76, 2012.

[54] J. Aguado, J. M. Arsuaga, A. Arencibia, M. Lindo, and V. Gascón, "Aqueous heavy metals removal by adsorption on amine-functionalized mesoporous silica," *Journal of Hazardous Materials,* vol. 163, pp. 213-221, 2009.

[55] M. Anbia, K. Kargosha, and S. Khoshbooei, "Heavy metal ions removal from aqueous media by modified magnetic mesoporous silica MCM-48," *Chemical Engineering Research and Design,* vol. 93, pp. 779-788, 2015.

[56] Y. Zhang, Y. Li, C. Dai, X. Zhou, and W. Zhang, "Sequestration of Cd (II) with nanoscale zero-valent iron (nZVI): characterization and test in a two-stage system," *Chemical Engineering Journal,* vol. 244, pp. 218-226, 2014.

[57] Y. Tang, S. Liang, J. Wang, S. Yu, and Y. Wang, "Amino-functionalized core-shell magnetic mesoporous composite microspheres for Pb (II) and Cd (II) removal," *Journal of Environmental Sciences,* vol. 25, pp. 830-837, 2013.

[58] Y. Zhu, J. Hu, and J. Wang, "Competitive adsorption of Pb(II), Cu(II) and Zn(II) onto xanthate-modified magnetic chitosan," *Journal of Hazardous Materials,* vol. 221-222, pp. 155-161, 2012.

[59] F. An, B. Gao, X. Dai, M. Wang, and X. Wang, "Efficient removal of heavy metal ions from aqueous solution using salicylic acid type chelate adsorbent," *Journal of Hazardous Materials,* vol. 192, pp. 956-962, 2011.

[60] A. Adamczuk and D. Kołodyńska, "Equilibrium, thermodynamic and kinetic studies on removal of chromium, copper, zinc and arsenic from aqueous solutions onto fly ash coated by chitosan," *Chemical Engineering Journal,* vol. 274, pp. 200-212, 2015.

[61] L. Jiang, S. Li, H. Yu, Z. Zou, X. Hou, F. Shen, *et al.*, "Amino and thiol modified magnetic multi-walled carbon nanotubes for the simultaneous removal of lead, zinc, and phenol from aqueous solutions," *Applied Surface Science,* vol. 369, pp. 398-413, 2016.

[62] E. Asuquo, A. Martin, and P. Nzerem, "Evaluation of Cd (II) Ion Removal from Aqueous Solution by a Low-Cost Adsorbent Prepared from White Yam (Dioscorea rotundata) Waste Using Batch Sorption," *ChemEngineering,* vol. 2, p. 35, 2018.

[63] M. Temkin, "Kinetics of ammonia synthesis on promoted iron catalysts," *Acta physiochim. URSS,* vol. 12, pp. 327-356, 1940.

[64] F. Batool, J. Akbar, S. Iqbal, S. Noreen, and S. N. A. Bukhari, "Study of Isothermal, Kinetic, and Thermodynamic Parameters for Adsorption of Cadmium: An Overview of Linear and Nonlinear Approach and Error Analysis," *Bioinorganic chemistry and applications,* vol. 2018, 2018.